Large Fixture Calibration Method Based on Point Cloud Scanning for Robotic Drilling

1st Yongzhuo Gao
the State Key Laboratory of Robotics and System
Harbin Institute of Technology
Harbin, China
gaoyongzhuo@hit.edu.cn

2nd Haibo Gao
the State Key Laboratory of Robotics and System
Harbin Institute of Technology
Harbin, China
gaohaibo@hit.edu.cn

3nd Dexin Cheng
the State Key Laboratory of Robotics and System
Harbin Institute of Technology
Harbin, China
22B908047@stu.hit.edu.cn

4th Wei Dong
the State Key Laboratory of Robotics and System
Harbin Institute of Technology
Harbin, China
dongwei@hit.edu.cn

2024 9th International Conference on Automation, Control and Robotics Engineering (CACRE) | 979-8-3503-5030-2/24/$31.00 ©2024 IEEE | DOI: 10.1109/CACRE62362.2024.10635049

***Abstract*—The rocket fuel tank requires the splicing of multiple sub-parts, which is difficult to be processed in an integrated manner. Among them, the short shell parts of the storage tank play a linking role and need to be drilled on the surface. Due to the large size of the tooling of the parts, there are problems such as large installation and positioning errors and low precision of robot automatic drilling. Therefore, a robot automatic hole making calibration method is proposed to solve the current problems. In order to achieve automated control, a large-scale robot automatic drilling system must have large-scale flexible tooling, control algorithms, human-computer interaction interfaces, execution units, and integrated tool rooms. It is essential to build effective calibration procedures as a foundation for this automation. The calibration plane is fitted, positioned, and calibrated using the point cloud scanning method. Subsequently, the hand-eye calibration method is employed to establish the relationship between the coordinate systems. Using this approach, the calibration process is ultimately finished, resulting in the successful implementation of automated drilling. The experimental findings demonstrate that, in the designated quadrant, the drilling rate of the robot can achieve 5 holes per minute. Furthermore, the average variance of the hole position is below $0.2mm$, and the highest error is $0.5mm$. These results align with the requirements of practical production.**

***Index Terms*—rocket fuel tank, point cloud scanning, hand-eye calibration, automatic hole making**

I. Introduction

The launch vehicle's strength and reliability indicators are essential for successfully executing the national space planning mission, since it serves as the transportation vehicle into space [1]. There has been a substantial increase in the demand for rocket launch missions in our country.Nevertheless, within the aerospace industry, the assembly procedure for launch vehicle tank components has traditionally relied on manual workshop manufacturing methods. The inadequate efficiency has severely limited the manufacturing capacity of launch vehicles, thereby constraining the demand for satellite launches. Hence, in the scenario of high-volume, diverse, and adaptable manufacturing of aerospace goods, there is a pressing need to enhance the quality of critical components and increase production efficiency. Industrial robots has the benefits of effortless implementation, extensive production adaptability, and economical cost. They are becoming more and more prevalent in the aerospace sector, particularly in the process of creating riveting holes during traditional assembly procedures [2]. The part contains a quantity of riveting holes ranging from 400 to 500. The implementation of automated robotic systems for creating holes is highly important in enhancing product quality and streamlining production methods.

The foreign aviation sector has made early and rapid progress in the design and development of automatic hole-making systems, resulting in significant achievements. In the 1950s, the United States initiated the development of automated drilling and riveting machines, which were subsequently utilised in the fabrication of aircraft equipment. ELectroimpace, an American business, has successfully created the SA2 automatic drilling and riveting machine. This particular automated drilling and riveting machine is specifically engineered for the purpose of creating holes and performing riveting operations on A320 wing panels [3]. In the United States, EI has created a robotic autonomous drilling device called the one-sided cell end effector (ONCE) [4]. This technology achieves a drilling position accuracy of $0.25mm$. Compared with relatively mature robotic automatic hole-making systems abroad, my country started late in automatic hole-making technology. At present, the development and application of automatic hole making systems are mainly concentrated in many large domestic aviation manufacturing companies and universities [5]. The Beijing Aviation Manufacturing Engineering Research Institute and Shenyang Aircraft Industry Group have collaborated to develop a five-coordinate CNC automatic hole creating equipment. This equipment is specifically designed for the automatic hole making process in the flexible assembly

*Yongzhuo Gao, Email: gaoyongzhuo@hit.edu.cn

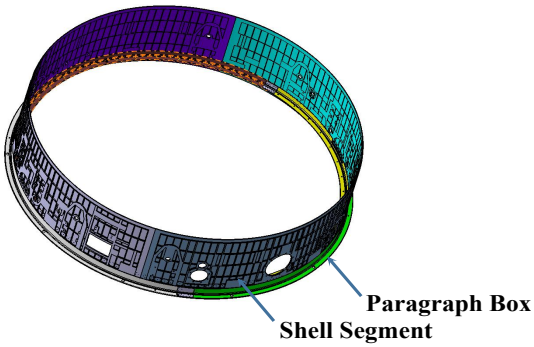

Fig. 1. Short shell component structure.

of aircraft wing parts [6]. Beihang University independently developed an automatic hole-making robot system consisting of spindle, feeding, pressing, connecting, sensing, control, vision and other units [7]. Domestic research on robotic automatic hole-making technology is still in the exploratory stage. Its applicability is poor, the requirements for hole-making accuracy are not high, and it is difficult to meet the application scenarios.

To address the aforementioned issues, the author suggested implementing a robotic automated hole-making technology for the small shell components of the rocket tank.

II. Adaptable tooling design

The launch vehicle short shell assembly comprises a shell segment and an end frame. The shell segment and the end frame are joined together using rivets during the assembling process. The total number of rows of rivets is 3. The structure of the short shell assembly is depicted in Fig. 1.

During the research, it was vital to carry out the hole forming procedure for short shell parts with three different diameters: 2900mm, 3350mm, and 3800mm. Consequently, a specialised tooling system was developed specifically for short shell components. This set of tooling consists of multiple backing plates, mounting plates, mounting ring components and clamping units. Several pads are evenly distributed on the turntable. An interposed mounting plate is positioned between two contiguous pads. The mounting ring assembly is affixed to the mounting plate. The mounting ring assembly is equipped with many evenly distributed clamping elements. Securely fasten the lower section of the small shell. Due to the substantial weight of the barrel section and the small size of the necessary holes, the drilling process is characterised by a rapid speed and a short duration. Thus, the adaptable tooling of the barrel section, built in this manner, guarantees the secure fastening and drilling of the barrel section.

In actual use, the short-shell flexible tooling has positioning functions, clamping functions and rotation functions. Its overall structure is shown in Fig. 2. The positioning function is achieved through the arrangement of three sets of wedge-shaped positioning blocks on the rotary table. The wedge-shaped positioning blocks serve the purpose of aligning and supporting the workpiece, and are effective in achieving accurate positioning. The clamping function is performed by a

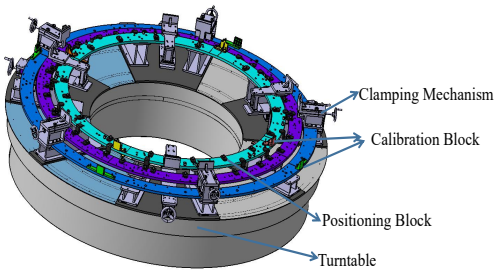

Fig. 2. Flexible tooling structure.

clamping unit on the positioning block, in which the clamping jaws rotate together with the workbench. The rotation function is executed by the turntable using the flexible tooling. The turntable utilises an internal gear transmission mechanism and is lubricated with semi-fluid grease. The collaboration between the robot and the turntable enables the drilling of holes on the whole surface of the workpiece in a 360° manner. The pressure plate restricts the vertical movement (Z-direction) of the workpiece, while the positioning pin restricts the movement of the workpiece in the horizontal plane (XY plane). Various workpieces are equipped with specific positioning pins and pressure plates located at different places.

III. PCL scanning

During the production process, the drilling of the part is accomplished by rotating the turntable in a specific direction. Conventional manual drilling necessitates manual placement, which can be challenging to ensure efficiency and accuracy due to the numerous drilling positions on the part. Although robot-assisted automated drilling has significantly enhanced drilling efficiency, it does not ensure placement precision. This is primarily due to the significant disparity between the turntable and the minor distortion of the parts built manually. To address these error sources, the methods of directional rotation of the turntable and laser calibration are used. In this article, we mainly take the 2900 specification short shell as an example to describe its calibration method. This calibration method is suitable for all parts processing.

A. Parts layout plan

Part splicing, manual assembly and micro-deformation of parts directly affect drilling accuracy. In order to reduce the impact of these aspects, a precise positioning plan for parts was developed, as shown in Fig. 3. The four quadrants on the turntable are carved with lasers to determine the initial position of the parts. Additionally, positioning pins on the edges of the

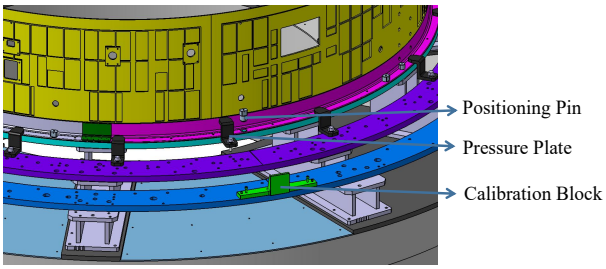

Fig. 3. Positioning layout diagram.

Algorithm 1 :2D Data Conversion

Data: (x_i, y_i)
Result: Point Cloud info (x_k, y_k, z_k)
Step 1:
(a) Define point cloud size
(b) Get robot speed V, Laser acquisition time t and Calibration block height h
Step 1:
(a) Calculate: $y_k = V \cdot t \cdot n, n = [0, \frac{h}{V \cdot t}]$,n represents the n^{th} contour
(b) Filter and Store data

parts ensure precise placement. To prevent any movement of the parts during the drilling process, a pressure plate is used to secure them. Due to the curved nature of the part's surface, it is necessary to guarantee that the axis of the electric spindle is parallel to the normal of the tangent plane when drilling on the surface of the part. Since the datum of the part needs to be determined when drilling to achieve automation, the datum of the part is set at the intersection of the quadrant and the part. In order to identify the quadrant position, it is necessary to set a calibration block at that position. This allows for the determination of the actual coordinate system and part datum of the calibration block. The following topic to be discussed is the examination of calibrating techniques.

B. Clibration algorithm

In order to obtain the actual coordinate system of the calibration block and the datum of the part, it is necessary to combine the robot base coordinate system W_b, the calibration block coordinate system W_m, the motorized spindle coordinate system W_z, the part datum coordinate system W_q, the laser sensor coordinate system W_s, and the flange center The coordinate system W_e is determined, as shown in Fig. 4. The coordinate system of the calibration block in the figure is the theoretical coordinate system. In this article, a 2-dimensional laser sensor is used to display a 3-dimensional calibration block plane, and the method is implemented in Algorithm 1. The obtained point cloud data is obtained based on the laser sensor scanning the calibration block, and the 3D data represents the surface position information of the calibration block. Since the point cloud is composed of discrete points without any specific patterns, it is not possible to directly determine the normal of the plane. Hence, it is necessary to perform plane fitting on all individual data points in order to determine the normal vector of the calibration block. The current coordinate system of the line and calibration block. Fig. 5 displays the distribution of the point cloud. Apply the least squares method to carry out plane fitting and derive the plane equation and normal vector of the fitted plane.

First, define the general equation of the plane:

$$Z = a \cdot X + b \cdot Y + c \tag{1}$$

For N discrete points($N > 3$) to fit the plane, there is a minimum value of P in the following equation (2).

$$P = \sum_{k=1}^{N} (a \cdot x_k + b \cdot y_k + c - z_k) \tag{2}$$

Secondly, in order to obtain the coefficients of the fitted plane equation, it is necessary to obtain partial derivatives of the coefficients separately and make the partial derivatives zero, that is:

$$\begin{cases} 2 \cdot \sum\limits_{k=1}^{N} (a \cdot x_k + b \cdot y_k + c - z_k) \cdot x_k = 0 \\ 2 \cdot \sum\limits_{k=1}^{N} (a \cdot x_k + b \cdot y_k + c - z_k) \cdot y_k = 0 \\ 2 \cdot \sum\limits_{k=1}^{N} (a \cdot x_k + b \cdot y_k + c - z_k) = 0 \end{cases} \tag{3}$$

To determine the relevant coefficients, the equation (3) needs to be transformed into matrix form.

$$\begin{bmatrix} \sum\limits_{k=1}^{N} x_k \cdot z_k \\ \sum\limits_{k=1}^{N} y_k \cdot z_k \\ \sum\limits_{k=1}^{N} z_k \end{bmatrix} = X \cdot \begin{bmatrix} \sum\limits_{k=1}^{N} x_k^2 & \sum\limits_{k=1}^{N} x_k \cdot y_k & \sum\limits_{k=1}^{N} x_k \\ \sum\limits_{k=1}^{N} x_k \cdot y_k & \sum\limits_{k=1}^{N} y_k^2 & \sum\limits_{k=1}^{N} y_k \\ \sum\limits_{k=1}^{N} x_k & \sum\limits_{k=1}^{N} y_k & N \end{bmatrix} \tag{4}$$

Finally, equation (4) is directly simplified to $AX = B$, where $x = [a, b, c]^T$. By considering the position of the discrete point in relation to the matrix A, we can determine the coefficients of the plane equation and the normal vector $n_p = (a, b, -1)$. This normal vector represents the calibration block's normal direction.

Currently, we only have information on the normal of the calibration block, but we do not know the exact coordinate system of the block. Fig. 6 introduces the theoretical calibration block coordinate system. To determine the real coordinate

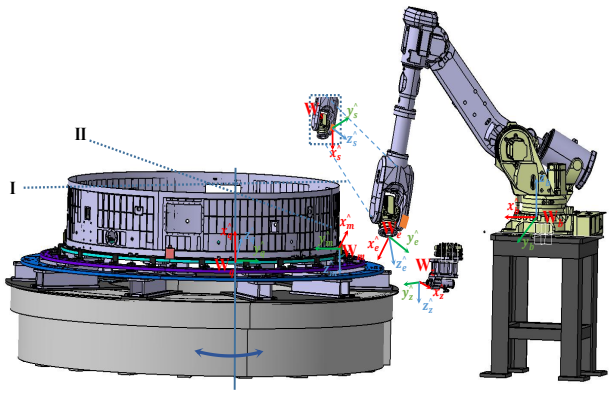

Fig. 4. Schematic diagram of coordinate system distribution.

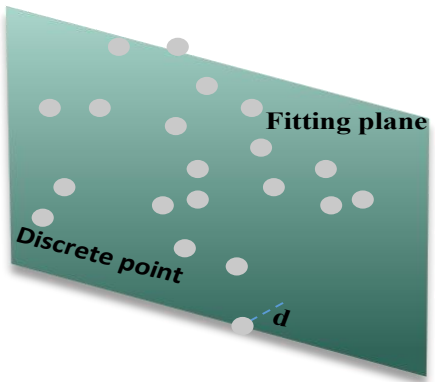

Fig. 5. Schematic diagram of coordinate system distribution.

Algorithm 2 :Coordinate Transformation

Data: T_q^m T_s^b T_q^z T_q^b (x_k, y_k, z_k)
Result: T_z^b
Step 1:
(a) Get the center position of the calibration block $(x_c, y_c, z_c) = \frac{1}{n} \cdot \sum_{i=1}^{n}(x_k, y_k, z_k)$
(b) Get the calibration block rotation matrix $[\vec{x}, \vec{y}, \vec{z}]$ and T_m^s
Step 1:
(a) Laser sensor pose matrix : $T_q^b = T_s^b \cdot T_m^s \cdot T_q^m$
(b) End effector pose matrix: $T_z^b = T_z^q \cdot T_q^b$

system, more computations are required, as outlined in Equation (5).

$$\begin{cases} \widehat{x}'_m = \widehat{z}_m \times n_p \\ \widehat{y}'_m = n_p \times \widehat{x}'_m \end{cases} \tag{5}$$

The theoretical z-axis component $\widehat{z} = (0, 0, 1)$ is defined as the basis for calculating the components of other axes using cross product calculations, as seen in Fig. 6.

Thus far, the precise coordinate system of the calibration block has been acquired. The part datum is determined using coordinate transformation, specifically by calculating the coordinates of the drilling origin relative to the robot base. Algorithm 2 implements the method.

IV. System Control Strategy

This robotic system automates the process of drilling short shell pieces. It includes several components such as an online detection system using a line laser scanner, trajectory calculation and generation performed by an industrial computer, and the use of an electric spindle tool for drilling. The industrial computer interfaces with the Programmable Logic Controller (PLC) controller and the robot control system via utilising robots, specific end effectors, and visual inspection equipment. The system's modules are linked to the PLC control system to achieve the mechanisation and automation of drilling and hole-making for short shell parts. This integration enhances the quality and efficiency of hole-making for short shell parts with barrel sections, as depicted in Fig. 7.

As shown in Fig. 8, the entire system adopts a distributed structure and has multiple control systems. The components include: industrial computer system (1), short-shell flexible tooling (2), electric spindle and drilling tool (3), robot control system (4), PLC control system (5), ABB robot (6), line laser scanner equipment (7) and turntable (8).

The industrial computer system uses an industrial computer, which uses the Modbus communication protocol with the lower computer PLC control system to transmit commands, and uses I/O signals to obtain the data results of the scanner for calculation, and finally generates the robot drilling trajectory and sends it to the ABB robot. The PLC control system enables immediate operation of the online inspection equipment (laser scanner), end drilling actuator (electric spindle and drilling tool), flexible tooling, and turntable. After receiving PLC instructions, the ABB robot carries out preset processing steps, including moving line laser scanner calibration, grasping and discharging spindle tools, and executing feed drilling programs. After receiving the PLC instruction, the turntable rotates the workpiece to the corresponding angle, thus making up for the limitations of the robot's workespace.

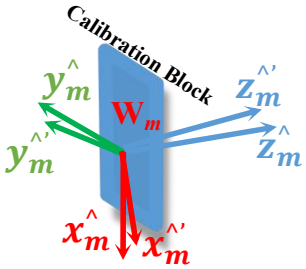

Fig. 6. Calibration block theoretical coordinate system.

V. Process and System Experiments

A. Experiment procedure

Within the drilling system, the robot's working space is unable to reach all positions needed to drill due to the huge size of the short-shell workpiece. Therefore, a turntable is necessary to modify the direction of the flexible tooling. Simultaneously, to guarantee precise positioning following rotation, the 360° short shell portion holes must be separated into four quadrants for processing. Every quadrant is furnished with a calibration block, and a line laser scanner is employed for meticulous calibration. Thus, the entire sequence of tasks in the system is as follows:

- The industrial computer processes the supplied drilling position coordinate file, identifies the appropriate programme number, and initiates the drilling operation.
- The industrial computer transmits commands to the PLC, which then regulates the turntable's rotation to a specific angle based on the drilling position's quadrant.
- Once the rotation is finished, the PLC initiates the line laser scanning programme. The ABB robot then proceeds to the specified location and scans the calibration block using a predetermined path.
- The industrial computer receives the scanning results to do calculations, develops the robot's processing route, and transmits it to the robot control system. Simultaneously, it provides instructions to the PLC for grabbing.
- The PLC transmits instructions to the ABB robot, which then proceeds to grasp the electric spindle tool. Once the

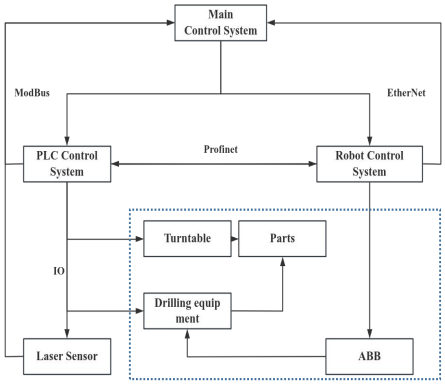

Fig. 7. Overall system control logic diagram.

speed is set, the electric spindle is activated to undergo preheating and attain its maximum speed.

- The ABB robot initiates ongoing drilling operations by following the designated processing trajectory and remains in communication with the PLC.
- After the drilling operation is complete, the PLC sends instructions to the ABB robot, which subsequently moves back to the intermediate location, indicating that the single hole processing method is ended.
- The turntable is reset, and the PLC awaits the next hole position information. This process is repeated until all hole positions are processed. Once this is done, the robot places the tool down, and the drilling is finished.

Fig. 9 illustrates the workflow of the automated drilling system implemented by the robot.

B. Results and Analysis

During the experimental validation, the electric spindle tool was outfitted with a $2.6mm$ drill bit. To guarantee a consistent feed quantity, a stratified feeding procedure was implemented. The primary process parameters are as follows: the number of layered feeds is 4, each feed amount is $3mm$, each retraction amount is $1mm$, the feed speed is $8mm/s$, the retraction speed is $60mm/s$, the adjustment speed is $150mm/s$, and the spindle speed is $4000r/min$.

The calibration block is shown in Fig. 10. The workpiece to be treated has a thickness of $10mm$. This process parameter can guarantee that the drilling depth fulfils the specified criteria. Throughout the grinding process, the robot consistently maintains a steady force state and a stable feed rate. Similarly, during regular drilling, the robot ensures that flying chips are evenly distributed and avoids any collisions or shaking, thereby ensuring safety.

The positioning accuracy of the hole was verified, and a vernier calliper was used to measure the positioning distance with an accuracy of $0.02mm$. The actual measurement results of the multiple hole positions after processing are shown in Fig. 10. The preset distance in the X direction is $20mm$, and the distance in the Y direction is $30mm$. It can be seen that the positioning accuracy of the $2.6mm$ drill bit is $0.4mm$.

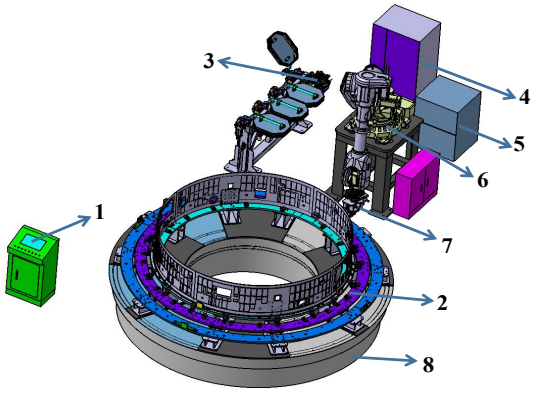

Fig. 8. Automatic drilling system layout.

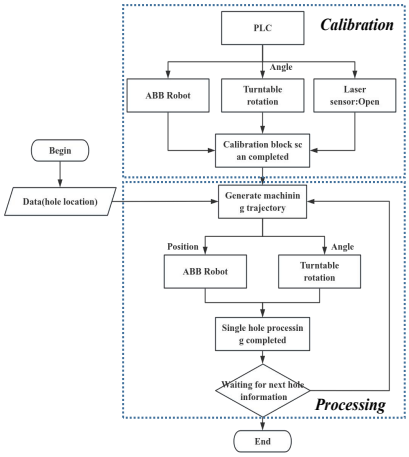

Fig. 9. Automatic drilling system layout.

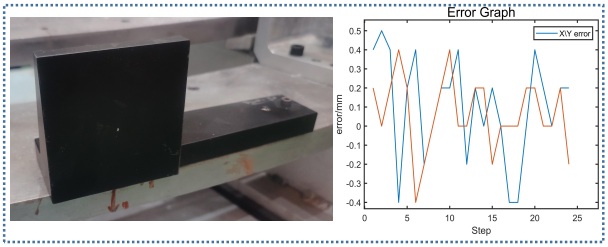

Fig. 10. Hole making effect and hole position error.

VI. Conclusion

In order to solve the problem of low efficiency and low precision in riveting hole making of rocket tank parts, the author completed the overall layout design of industrial robot automatic drilling equipment, flexible tooling design, calibration method, and other technologies, determined the optimal process parameters through process experiments, and verification was carried out on short shell prototypes. The verification results show that the system meets the application requirements of the model product and has the capability of engineering application.

References

[1] X. Wang and L. Xu, "Research on the development of new generation medium high-orbit launch vehicle in china," *Astronautical systems engineering technology*, vol. 9, 2019.

[2] M. Li, Z. Du, W. Dong, K. Gao, Y. Gao, and D. Wu, "Modeling, planning, and control of robotic grinding on free-form surface using a force-controlled belt grinding tool," *Proceedings of the Institution of Mechanical Engineers, Part C: Journal of Mechanical Engineering Science*, vol. 236, no. 4, pp. 2009–2028, 2022.

[3] R. DeVlieg, K. Sitton, E. Feikert, and J. Inman, "Once (one-sided cell end effector) robotic drilling system," SAE Technical Paper, Tech. Rep., 2002.

[4] A. Frommknecht, J. Kuehnle, I. Effenberger, and S. Pidan, "Multi-sensor measurement system for robotic drilling," *Robotics and Computer-Integrated Manufacturing*, vol. 47, pp. 4–10, 2017.

[5] Q. Quan, T. Wang, H. Yu, Q. Deng, D. Tang, and Z. Deng, "An ultrasonic drilling system for fast drilling speed with uncertain load," *IEEE/ASME Transactions on Mechatronics*, 2022.

[6] Zhou, Zou, Xue, Gan, and Du, "Research on automatic drill with five axes for flexible assembly of aircraft wing components," *Aeronautical Manufacturing Technology*, vol. 53, no. 2, pp. 44–46, 2010.

[7] W. T. e. a. GONG Maozhen, YUAN Peijiang, "Intelligent verticality-adjustment method of end-effector in aeronautical drilling robot," Master's thesis, 2012.